Nuclear Science and Techniques (2023) 34:9
https://doi.org/10.1007/s41365-022-01153-4

Investigation of β^{-}-decay half-life and delayed neutron emission with uncertainty analysis

Yu-Feng Gao[1,2,3] · **Bo-Shuai Cai**[3] · **Cen-Xi Yuan**[3]

Received: 13 September 2022 / Revised: 25 October 2022 / Accepted: 14 November 2022 / Published online: 18 January 2023

Abstract
β-decay half-life and β-delayed neutron emission (βn) are of great importance in the development of basic science and industrial applications, such as nuclear physics and nuclear energy, where β^{-}-decay plays an important role. Many theoretical models have been proposed to describe β-decay half-lives, whereas the systematic study of βn is still rare. This study aimed to investigate β^{-}-decay half-lives and βn probabilities through analytical formulas and by comparing them with experimental data. Analytical formulas for β^{-}-decay properties have been proposed by considering prominent factors, that is, decay energy, odevity, and the shell effect. The bootstrap method was used to simultaneously evaluate the total uncertainty on calculations, which was composed of statistic and systematic uncertainties. β^{-}-decay half-lives, βn probabilities, and the corresponding uncertainties were evaluated for the neutron-rich region. The experimental half-lives were well reproduced. Additional predictions are also presented with theoretical uncertainties, which helps to better understand the disparity between the experimental and theoretical results.

Keywords Neutron-rich nucleus · β-delayed neutron emissions · Bootstrap method

1 Introduction

The β-decay of exotic nuclei, especially approaching the proton dripline [1–3] and neutron dripline [4–6], has been focused on in recent decades. The development of experimental setups and techniques [7–9] provides more experimental data for theoretical investigations and enables more theoretical research tools [10–12]. However, estimating the related properties with satisfactory accuracy remains a challenge owing to the complexity of the nuclear structure and interactions between nucleons [5].

The study of β^{-}-decay and β^{-}-delayed neutron emission (βn) is of great importance in the development of both basic nuclear physics [13–15] and applied nuclear physics [16, 17]. In parameterizing the observed properties of atomic nuclei, some studies used quasiparticle random phase approximation based on energy density functionals [18–20] or semi-empirical models [21–23], while others have proceeded from a microscopic perspective, such as interacting bosons models [24–26] and the Hartree–Fock–Bogoliubov framework [27–30]. Such microscopic calculations, even with certain approximations on interactions and/or wavefunctions, are still time-consuming. Neat and reliable formulas are beneficial for the study of β-decay. Phenomenological models have been successively proposed for β^{-}-decay [31–33].

Along with the development of high-precision experimental techniques, we are gradually compensating for the deficiency in experimental data on β^{-}-decay [34–36], especially for nuclei near the neutron shell closures of 50 and 82 [37–39]. Therefore, a new systematic study is of interest

This work was supported by the Guangdong Major Project of Basic and Applied Basic Research (No. 2021B0301030006), and computational resources from Sun Yat-Sen University and the National Supercomputer Center in Guangzhou.

✉ Cen-Xi Yuan
yuancx@mail.sysu.edu.cn

1 Institute of Modern Physics, Chinese Academy of Sciences, Lanzhou 730000, China

2 School of Nuclear Science and Technology, University of Chinese Academy of Sciences, Beijing 100049, China

3 Sino-French Institute of Nuclear Engineering and Technology, Sun Yat-Sen University, Zhuhai 519082, China

and helps to understand β^--delayed neutron emission more comprehensively with reliable calculations.

This study focused on the β^--decay half-life $T_{1/2}$ and βn probability $P_{\beta n}$ of neutron-rich nuclei. Analytical formulas for the β^--decay strength are proposed based on standard β-decay theory with further physics considerations on decay energy, odevity, and the shell effect. Moreover, the bootstrap method was used to evaluate the uncertainties on calculations.

According to previous studies on β^--decay, the contribution of the first-forbidden (FF) transition to the total decay rate has been found as not negligible for nuclei far from the β-stable valley [23, 40, 41]. Note that we equated FF branches and other forbidden transitions to one or two effective Gamow–Teller (GT) branches in this study. For a better evaluation of β^--delayed neutrons, this study was only concerned with neutron-rich nuclei with $Z = 29\sim57$, which included important fission products and the precursors of the delayed neutron in the nuclear reactor [42]. The experimental data used for this study were taken from the newest compilation and evaluation of β-delayed neutron emission probabilities and half-lives for $Z > 28$ precursors provided by the AME-2020 [36, 43].

The main purposes of this study were to determine the parameters of the analytical formulas to describe $T_{1/2}$ and $P_{\beta n}$, to estimate the uncertainties on corresponding formulas using the bootstrap method, and to make predictions for nuclei without experimental data on $T_{1/2}$ and $P_{\beta n}$.

2 Methods

2.1 Theoretical derivation and formulas

In this study, we investigated the half-lives of the β^--decay and βn probabilities of neutron-rich nuclei. According to Fermi's β-decay theory, the standard formula of the β^--decay half-life $T_{1/2}$ through the Fermi and GT transitions is as follows [44]:

$$T_{1/2} = \frac{\kappa}{f_0(B_{\rm F} + B_{\rm GT})}, \tag{1}$$

where $\kappa \equiv \frac{2\pi^3\hbar^7 \ln 2}{m_e^5 c^4 G_F^2} = 6147$ s, $B_{\rm F}$ and $B_{\rm GT}$ are the reduced transition probability term for the Fermi and GT transitions, respectively, and f_0 is the phase-space factor, also known as the Fermi integral.

With the Primakoff–Rosen approximation [45] applied to f_0, Eq. (1) was simplified to a manipulable form, which also imposed a relatively high value of the β-decay energy Q_β for the constraint on the selection of experimental data. All nuclei in this study were selected with Q_β greater than 3 MeV, taken from a new compilation [36, 43]. All other branches were equated to one or two effective GT branches, and a logarithmic formula was derived from Eq. (1) with the same notations as in Eq. (2) in removing the term $B_{\rm F}$.

$$-\ln(B_{\rm GT}) = -\ln(\kappa) + \ln\left[\frac{2\pi\alpha Z_{\rm f}}{1-\exp(-2\pi\alpha Z_{\rm f})}\right] + \ln(T_{1/2}) + \ln\left(\frac{1}{30}(E_0^5 - 10E_0^2 + 15E_0 - 6)\right), \tag{2}$$

where $E_0 \equiv \frac{E_{\rm i}-E_{\rm f}}{m_e c^2}$, $E_{\rm i}$ and $E_{\rm f}$ are the energy levels of the initial and final states, respectively, whose difference $(E_{\rm i} - E_{\rm f})$ is consequently the decay energy Q_β, and $Z_{\rm f}$ is the number of protons of the daughter nucleus.

Subsequently, a linear formula describing $-\ln(B_{\rm GT})$ was established based on physical meanings. After β-decay, an odd-odd (oo) nucleus decays into an even-even (ee) nucleus, whereas an odd-A (oA) nucleus decays into another oA nucleus. Q_β, calculated from ground state to ground state, does not necessarily reflect the actuality of E_0 of the effective branch. Thus, multiplicative factors were introduced to include the odevity in E_0. Moreover, the oo nucleus more likely decays into the excited state of the ee nucleus for small effective decay energies because the angular momentum of the ground state of the oo parent nucleus tends to differ significantly from that of the ground state of the ee daughter nucleus. With a similar analysis for the case of oA and ee nuclei, there is a pronounced stratification of reduced transition intensities of the three types owing to the different magnitudes of the multiplicative factors.

Considering Eq. (2) and the differences in effective decay energy owing to different odevities, a new formula was accordingly constructed for $-\ln(B_{\rm GT})$ with the Dirac function,

$$-\ln(B_{\rm GT}) = a_0 + a_1\delta_{\rm oA} + a_2\delta_{\rm oo}. \tag{3}$$

The Dirac functions $\delta_{\rm oo}$ and $\delta_{\rm oA}$ can discern the odevity. The corresponding term for ee nuclei was set as a constant, a_0. Furthermore, the pronounced peaks of the $-\ln(B_{\rm GT})$ values observed in the distribution of experimental data are bound up with the periodic arrangement of the nuclei, namely, the shell effect of the nucleus. Therefore, a correction term, a_3x_3, for the shell effect was added,

$$-\ln(B_{\rm GT}) = a_0 + a_1\delta_{\rm oA} + a_2\delta_{\rm oo} + a_3x_3, \tag{4}$$

where a_0, a_1, a_2, and a_3 are fitting parameters, $x_3 = \sum_{N_k,Z_k} \exp\left[-\left(\frac{N-N_k}{5}\right)^2 - \left(\frac{Z-Z_k}{5}\right)^2\right]$, and N_k and Z_k describe the shell and sub-shell structures and were chosen to be (50, 32) and (82, 50) according to the locations of distinct peak points.

Equations (3) and (4) can only describe a single decay branch without considering the βn branch. In the below content, βo denotes the branch that is not βn. The relations between β-decay half-life and βn probability are as follows:

$$P_{\beta n} + P_{\beta \mathrm{o}} = 1, \tag{5}$$

$$\frac{1}{T_{1/2}} = \frac{1}{T_{\beta n}} + \frac{1}{T_{\beta \mathrm{o}}}, \tag{6}$$

$$-\ln P_{\beta n} = -\ln\left(\frac{T_{1/2}}{T_{\beta n}}\right), \tag{7}$$

$$-\ln\left(\frac{P_{\beta n}}{1-P_{\beta n}}\right) = -\ln\left(\frac{T_{\beta \mathrm{o}}}{T_{\beta n}}\right), \tag{8}$$

where $T_{\beta n}$ ($T_{\beta \mathrm{o}}$) and $P_{\beta n}$ ($P_{\beta \mathrm{o}}$) denote the partial half-life and probability of the βn (βo) branch. Thus, an analogical formula could be proposed for $-\ln(P_{\beta n})$ with a new optimizing term for the effect of the difference between $Q_{\beta n}$ and Q_β on the βn probability,

$$-\ln(P_{\beta n}) = a_0 + a_1\delta_{\mathrm{oA}} + a_2\delta_{\mathrm{oo}} + a_3x_3 + a_4x_4, \tag{9}$$

where $x_4 = \ln\left(\frac{Q_{\beta n}}{m_e c^2}\right) - \ln\left(\frac{Q_{\beta \mathrm{o}}}{m_e c^2}\right)$, and $Q_{\beta n}$ ($Q_{\beta \mathrm{o}}$) denotes the decay energy of the βn (βo) branch from ground state to ground state. This makes use of a direct logarithmization of $P_{\beta n}$, yet it may obtain nonphysical results during fitting, that is, $P_{\beta n} > 1$. $P_{\beta n}$ was replaced by $\frac{P_{\beta n}}{1-P_{\beta n}}$ to avoid such results, and the derived formula is expressed as

$$-\ln\left(\frac{P_{\beta n}}{1-P_{\beta n}}\right) = a_0 + a_1\delta_{\mathrm{oA}} + a_2\delta_{\mathrm{oo}} + a_3x_3 + a_4x_4. \tag{10}$$

2.2 Bootstrap method

This study evaluated the fitting parameters and uncertainties of β^--decay half-lives and βn probabilities by applying the bootstrap method. In applied statistics, the bootstrap method was proposed by Efron Bradley in 1985 [46] and used to determine the accuracy of estimating the unknown parameters of a chosen estimator through the basic idea of resampling [47].

After the first proposal of its application on alpha decay laws [47], it was successfully applied to the uncertainty determination of nuclear mass models [48, 49], proton decay stability [49], and the binary cluster model [50].

Similar to Monte Carlo events, a new dataset was obtained by resampling with replacements from a given experimental dataset. A group of parameters in the model was obtained by minimizing the root-mean-square of the residuals. Repeating this process M times, the total uncertainty was thus

$$\sigma_{\mathrm{tot}} = \sqrt{\frac{1}{MK}\sum_{m,k}(r_{m,k})^2}, \tag{11}$$

where m denotes the mth resampling of the dataset, k denotes the kth nucleus in the original dataset among the K nuclei, and $r_{m,k}$ is the residual between the observed value and its estimated value from the mth replication of bootstrap for the kth nucleus.

The total uncertainty was then decomposed into the statistical uncertainty σ_{stat} and systematic uncertainty σ_{sys}, which can be written as

$$\sigma_{\mathrm{stat}} = \sqrt{\frac{1}{(M-1)K}\sum_{m,k}(r_{m,k}-\bar{r}_k)^2}, \tag{12}$$

$$\sigma_{\mathrm{sys}} = \sqrt{\frac{1}{K}\sum_k\left(\frac{1}{M}\sum_m r_{m,k}\right)^2}. \tag{13}$$

In this study, this method was used to assess the uncertainty on Eqs. (3), (4), (9), and (10). The global systematic uncertainty of model deficiency, σ_{sys}, and the statistical uncertainty appropriate to the specific nucleus were combined to evaluate the confidence interval.

$$\sigma_{\mathrm{pred},k} = \sqrt{\sigma^2_{\mathrm{stat},k} + \sigma^2_{\mathrm{sys}}} \tag{14}$$

Because the reduced transition probability term and the probabilities of the βn and βo branches were in the logarithmic form, the uncertainties obtained were propagated to be different positive and negative deviations when the half-lives and probabilities were further calculated.

3 Results and discussion

Next, the half-life of β^- decay and the probability of occurrence of βn decay were investigated using two experimental datasets and several previously proposed formulas. The bootstrap method was used to deal with the uncertainty analysis.

3.1 One effective decay branch

Nuclei were carefully selected from the newest compilation and evaluation with experimental half-lives smaller than 2 s and Q greater than 3 MeV because forbidden transitions may dominate long-lived transitions and are not suitable for study as effective GT branches. Nuclei with βn basically meet these two conditions. Among 256 selected nuclei, two datasets were taken: one containing all 256, which have half-life measurements, and the other containing 133, which have βn probability measurements.

Based on the assumption of one effective decay, the bootstrap method was used to investigate the first dataset, as listed in Table 1. The shell effect did contribute to the description of half-lives, as indicated by the decreasing systematic uncertainty. Figure 1 shows the results of the difference between the observed data and calculation corresponding to Eqs. (3) and (4). In general, the latter with the shell effect reproduced better than the former, especially where the major shell and sub-shell closures were located.

3.2 Two effective decay branches

Then, we considered the case in which there are neutron emissions after β decay, that is, two decay branches with βn emitting neutrons and βo without emitting. It should be noted that there is no distinction between the number of neutrons emitted. Equation (4) was applied to each branch with the second dataset. The corresponding results are listed in the last two lines of Table 2 with the notations Eqs. $(4)_{\beta n}$ and $(4)_{\beta o}$.

Moreover, the one-branch result was re-fitted to compare the adaptability of Eq. (4) with the changed dataset. The values of βn probability largely varied from nuclide to nuclide, resulting in larger uncertainties in Eqs. $(4)_{\beta n}$ and $(4)_{\beta o}$ compared with $1b4p$.

The values of $-\ln(B_{\mathrm{GT}})$ were calculated to deduce the partial half-life of the two branches, $T_{\beta n}$ and $T_{\beta o}$, then the $T_{1/2}$

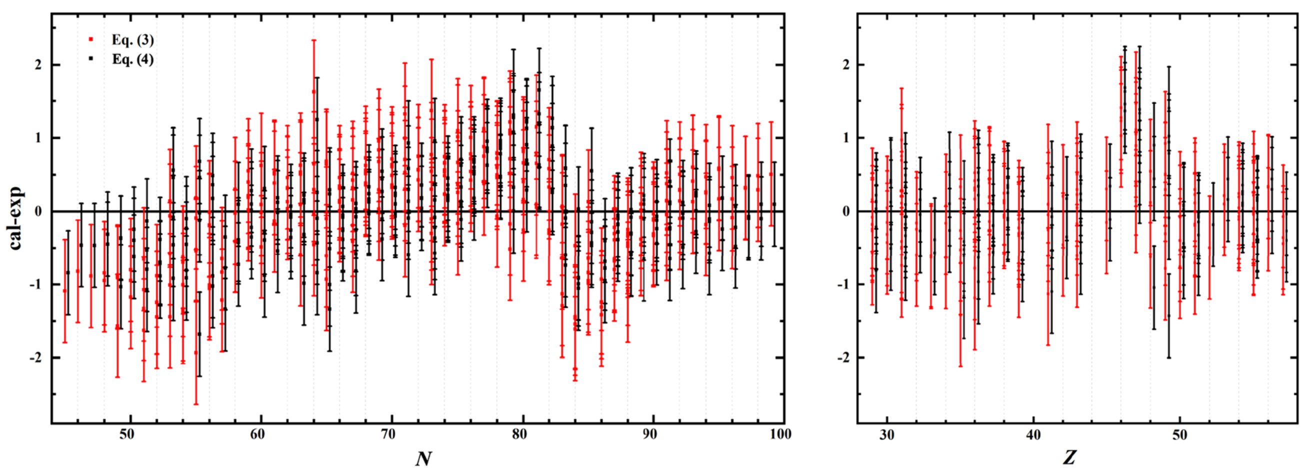

Fig. 1 Distribution of the difference between the calculated values and experimental values of $\ln T$ with error bars. In the one-branch case, the red and black squares correspond to Eq. (3) with three parameters and Eq. (4) with four parameters, respectively

Table 1 Mean values of fitting parameters corresponding to Eqs. (3)and (4) using the first dataset. The three columns σ^2_{stat}, σ^2_{sys}, and σ^2_{tot} show the square of the statistical, systematic, and total uncertainties, respectively

	Fitting parameters				Uncertainties		
	a_0	a_1	a_2	a_3	σ^2_{stat}	σ^2_{sys}	σ^2_{tot}
Equation (3)	0.8938	1.0489	1.9296	–	0.0059	0.4887	0.4946
Equation (4)	0.5053	1.0450	1.9081	0.9459	0.0053	0.3226	0.3278

Table 2 Mean values of fitting parameters corresponding to Eq. (4) with four parameters and the one branch assumption, and with the two decay branches separately, Eqs. $(4)_{\beta n}$ and $(4)_{\beta o}$, using the second dataset

	Fitting parameters				Uncertainties		
	a_0	a_1	a_2	a_3	σ^2_{stat}	σ^2_{sys}	σ^2_{tot}
Equation (4)	0.3649	1.0179	2.0070	1.0725	0.0079	0.2565	0.2644
Equation $(4)_{\beta n}$	0.4384	0.6672	0.9952	0.3666	0.0255	0.8433	0.8687
Equation $(4)_{\beta o}$	0.6838	1.1007	1.9844	1.4825	0.0131	0.4428	0.4559

appearing in Eqs. (6) and (7), and the branching ratios. The experimental half-lives were generally well reproduced. In particular, the shorter the half-life, the better the consistency.

The root-mean-square deviation (RMS), which characterizes the goodness-of-fit of one dataset, is defined as

$$\mathrm{RMS} = \frac{1}{K}\sum_{k=1}^{K}[Y_{k,\mathrm{cal}} - Y_{k,\mathrm{exp}}]^2. \tag{15}$$

The results obtained by direct fitting to the βn probability are listed in Table 3. The three results and experimental values were generally consistent within approximately 10% RMS (10.389%, 10.002%, and 10.231%, respectively).

The value given by $-\ln(P_{\beta n})$ was close to the experimental value in general. However, the $-\ln\left(\frac{P_{\beta n}}{1-P_{\beta n}}\right)$ results were closer to the experimental data in several cases with great undulations, such as in the regions of shell closure. The form of $-\ln\left(\frac{P_{\beta n}}{1-P_{\beta n}}\right)$ was determined in a more physical transformation, guaranteeing that the calculated probabilities always lay between 0 and 1.

The experimental and calculated values of the half-life and probability are shown in Table 4 for the two-branch case. The calculated values of the half-life were obtained from the fitting results of Eqs. $(4)_{\beta n}$ and $(4)_{\beta \mathrm{o}}$ listed in Table 2, whereas the probability corresponds to Eq. (9) listed in Table 3.

Because the uncertainties were estimated on a logarithmic scale, the distances from the upper and lower bounds to the predicted values were different when converting, and thus there were differences in the positive and negative directions of the uncertainties.

For the sake of convenience, the half-lives are presented in natural logarithmic form with T in units of seconds so that the total uncertainty on the calculated values can be given in the same scale in the sixth column. Because the two formulas Eqs. (9) and (10) study different objects, the calculated values of probability were converted from the natural logarithm form.

3.3 Predictions

According to the presented method, the predictions of β-decay half-lives and βn probabilities $P_{\beta n}$ could be given for nuclei without experimental data, and the uncertainties according to Eq. (14). The predictions for neutron-rich nuclei in the intermediate mass zone offer important nuclear input and relevant data for nuclear physics applications, such as fission product yields in nuclear reactors [16], and the half-lives of nuclei participating in the rapid neutron capture process (r process) in astrophysics [51].

In Table 5, 123 nuclei without experimental values of $P_{\beta n}$ are listed, 18 of which also have no half-life (in the last eighteen lines of the table). The predictions corresponding to Eqs. (10) and (4) are given for the probability and half-life, respectively.

4 Conclusion

This study focused on the properties of β-decay, that is, the half-lives and probability of releasing the delayed neutrons of neutron-rich nuclei with atomic numbers from 29 to 57, which are important fission products. During the review phase of the paper, new experimental results were published [52]. Taking experimental uncertainty into account, the latest results are all within one standard deviation of our prediction, with an RMS equal to 16.752%.

In considering the odevity as well as the shell effect, phenomenological formulas for β-decay were proposed on top of the classical formula. The β-decay neutron emission (βn) probability has a similar formula to the half-life based on their relationship analysis, except for the addition of new terms to include the differences between the decay energy when releasing delayed neutrons and that of not.

Based on the fitting results, the β-decay half-lives, βn probabilities, and the corresponding uncertainties were calculated. The experimental half-lives were generally well reproduced. In particular, the shorter the half-life, the better the consistency. An uncertainty analysis of the β-decay formula was successfully performed using the bootstrap method. In this way, the uncertainties on the theoretically predicted values were obtained, which helps to better understand the disparity between experimental and theoretical results and predict the β-decay half-lives and βn probabilities of nuclei without experimental data.

Table 3 Mean value of fitting parameters corresponding to Eqs. (9) and (10) using the second dataset. The three columns σ^2_{stat}, σ^2_{sys}, and σ^2_{tot} show the square of the statistical, systematic, and total uncertainties, respectively

	Fitting parameters					Uncertainties		
	a_0	a_1	a_2	a_3	a_4	σ^2_{stat}	σ^2_{sys}	σ^2_{tot}
Equation (9)	0.1956	−0.2570	−0.7434	−0.7137	−3.9323	0.0287	0.6966	0.7253
Equation (10)	−0.2697	−0.3780	−0.8663	-1.0562	−4.4410	0.0307	0.7492	0.7800

Table 4 Experimental and calculated values of the half-life and probability for the two-branch case. Q_β and $Q_{\beta n}$ are the decay energy of β-decay and βn-decay, respectively, in keV. $\ln T_{\mathrm{cal}}$ and P_{cal} are calculated using Eqs. (4) and (10). The uncertainties are given in one standard deviation, estimated using the bootstrap method

Nucl.	Q_β	$Q_{\beta n}$	$\ln T_{\mathrm{exp}}$	$\ln T_{\mathrm{cal}}$	$\sigma_{\ln T_{\mathrm{cal}}}$	$P_{\mathrm{exp}}(\%)$	$P_{\mathrm{cal}}(\%)$
$^{74}_{29}$Cu	9750.5	1515.9	0.469	0.254	0.573	0.075	$0.17^{-0.10}_{+0.24}$
$^{75}_{29}$Cu	8087.6	3214.1	0.202	0.33	0.575	2.7	$6.84^{-3.88}_{+8.19}$
$^{76}_{29}$Cu	11327	3511.6	−0.451	−0.232	0.575	7.2	$4.16^{-2.39}_{+5.29}$
$^{77}_{29}$Cu	10170	5610	−0.755	−0.766	0.574	30.1	$26.95^{-13.61}_{+19.98}$
$^{78}_{29}$Cu	12990	6220	−1.104	−0.969	0.573	51	$25.10^{-12.84}_{+19.46}$
$^{79}_{29}$Cu	11690	7670	−1.422	−1.647	0.573	66	$45.82^{-19.68}_{+21.08}$
$^{80}_{29}$Cu	15450	9160	−2.178	−2.143	0.572	58	$46.40^{-19.82}_{+21.02}$
$^{81}_{29}$Cu	14780	12160	−2.615	−3.428	0.574	81	$68.53^{-20.77}_{+15.30}$
$^{79}_{30}$Zn	9115.4	2202.3	−0.293	0.102	0.58	1.75	$0.98^{-0.58}_{+1.41}$
$^{80}_{30}$Zn	7575.1	2827.8	−0.576	−0.153	0.584	1.36	$4.52^{-2.60}_{+5.77}$
$^{81}_{30}$Zn	11428.3	4952.7	−1.205	−1.08	0.578	18	$11.75^{-6.52}_{+12.56}$
$^{82}_{30}$Zn	10616.8	7242.7	−1.727	−2.234	0.579	69	$40.15^{-18.30}_{+21.53}$
$^{84}_{30}$Zn	12160	9260	−2.926	−3.177	0.579	73	$50.33^{-20.59}_{+20.47}$
$^{80}_{31}$Ga	10311.6	2232	0.642	0.388	0.578	0.9	$0.99^{-0.58}_{+1.38}$
$^{81}_{31}$Ga	8663.7	3836	0.196	0.209	0.577	12.5	$12.85^{-7.09}_{+13.37}$
$^{82}_{31}$Ga	12484.3	5289.6	−0.509	−0.688	0.575	22.7	$16.48^{-8.89}_{+15.67}$
$^{83}_{31}$Ga	11719.3	8086.6	−1.171	−1.814	0.573	67	$51.24^{-20.68}_{+20.26}$
$^{84}_{31}$Ga	14060	8820	−2.352	−1.859	0.572	47.6	$52.66^{-20.89}_{+20.00}$
$^{85}_{31}$Ga	13270	10230	−2.387	−2.72	0.574	81.3	$62.76^{-21.34}_{+17.31}$
$^{86}_{31}$Ga	15320	10970	−3.012	−2.666	0.573	85.2	$66.10^{-21.11}_{+16.20}$
$^{87}_{31}$Ga	14830	12080	−3.54	−3.448	0.574	91.2	$67.57^{-20.91}_{+15.66}$
$^{84}_{32}$Ge	7705.1	3449.6	−0.049	−0.32	0.582	10.6	$9.60^{-5.39}_{+10.82}$
$^{85}_{32}$Ge	10065.7	4658.8	−0.699	−0.542	0.577	16.2	$15.22^{-8.28}_{+14.96}$
$^{86}_{32}$Ge	9560	5720	−1.505	−1.55	0.579	45	$27.79^{-14.00}_{+20.29}$
$^{86}_{33}$As	11541	5380.2	−0.058	−0.449	0.573	34.5	$22.93^{-11.90}_{+18.72}$
$^{87}_{33}$As	10808.2	6813.9	−0.726	−1.293	0.573	15.4	$40.82^{-18.43}_{+21.43}$
$^{88}_{34}$Se	6831.8	1936.2	0.412	0.148	0.583	0.99	$1.24^{-0.73}_{+1.73}$
$^{89}_{34}$Se	9281.9	3652.3	−0.821	−0.323	0.576	7.8	$6.95^{-3.95}_{+8.32}$
$^{91}_{34}$Se	10530	5350	−1.309	−1.207	0.572	21	$16.97^{-9.11}_{+15.91}$
$^{90}_{35}$Br	10959	4464.2	0.648	−0.517	0.571	25.6	$10.76^{-5.97}_{+11.66}$
$^{91}_{35}$Br	9866.7	5780.6	−0.609	−1.216	0.57	30.4	$25.02^{-12.77}_{+19.35}$
$^{92}_{35}$Br	12536.5	6669.8	−1.097	−1.619	0.569	33.1	$24.14^{-12.41}_{+19.11}$
$^{93}_{35}$Br	11250	7810	−1.884	−2.298	0.568	64	$36.52^{-17.10}_{+21.34}$
$^{94}_{35}$Br	13950	8670	−2.659	−2.548	0.568	30	$34.36^{-16.43}_{+21.27}$
$^{92}_{36}$Kr	6003.1	904.4	0.61	−0.022	0.578	0.0332	$0.04^{-0.03}_{+0.07}$
$^{93}_{36}$Kr	8483.9	2565.1	0.25	−0.716	0.569	1.99	$1.26^{-0.74}_{+1.74}$
$^{94}_{36}$Kr	7215	3201	−1.556	−1.218	0.577	1.11	$4.17^{-2.41}_{+5.37}$
$^{95}_{36}$Kr	9733	4333	−2.172	−1.643	0.569	2.87	$5.66^{-3.22}_{+6.94}$
$^{96}_{36}$Kr	8275	4741	−2.526	−2.098	0.576	3.7	$10.70^{-5.99}_{+11.82}$
$^{97}_{36}$Kr	11100	5860	−2.779	−2.436	0.568	6.7	$10.51^{-5.84}_{+11.47}$
$^{98}_{36}$Kr	10060	6140	−3.147	−3.123	0.576	7	$13.05^{-7.23}_{+13.65}$
$^{99}_{36}$Kr	12360	7540	−3.297	−3.076	0.568	11	$17.75^{-9.49}_{+16.34}$
$^{95}_{37}$Rb	9228	4883	−0.973	−1.533	0.568	8.8	$10.94^{-6.07}_{+11.81}$
$^{96}_{37}$Rb	11569.8	5693.9	−1.601	−1.799	0.569	14.1	$12.23^{-6.76}_{+12.89}$
$^{97}_{37}$Rb	10062.3	6333.7	−1.778	−2.133	0.568	24.9	$19.96^{-10.53}_{+17.44}$
$^{98}_{37}$Rb	12054	6141	−2.163	−2.056	0.57	14.354	$13.58^{-7.46}_{+13.88}$
$^{99}_{37}$Rb	11400.3	7230.6	−2.851	−2.752	0.568	19.1	$20.25^{-10.67}_{+17.58}$

Table 4 (continued)

Nucl.	Q_β	$Q_{\beta n}$	$\ln T_{\rm exp}$	$\ln T_{\rm cal}$	$\sigma_{\ln T_{\rm cal}}$	$P_{\rm exp}(\%)$	$P_{\rm cal}(\%)$
$^{100}_{37}$Rb	13574	8203	−2.976	−2.775	0.569	5.75	$24.98^{-12.83}_{+19.51}$
$^{101}_{37}$Rb	12480	8910	−3.474	−3.318	0.568	28	$29.98^{-14.81}_{+20.63}$
$^{102}_{37}$Rb	14450	9550	−3.297	−3.195	0.569	18	$33.11^{-16.04}_{+21.23}$
$^{97}_{38}$Sr	7540	1683.1	−0.846	−0.594	0.569	0.03	$0.25^{-0.15}_{+0.36}$
$^{98}_{38}$Sr	5871.7	1627	−0.426	−0.543	0.579	0.23	$0.44^{-0.26}_{+0.63}$
$^{99}_{38}$Sr	8128.4	1702.1	−1.313	−0.959	0.569	0.096	$0.18^{-0.11}_{+0.27}$
$^{100}_{38}$Sr	7506	2757.6	−1.606	−1.699	0.578	1.11	$1.51^{-0.89}_{+2.10}$
$^{101}_{38}$Sr	9736	3931	−2.163	−1.842	0.569	2.52	$3.29^{-1.90}_{+4.29}$
$^{102}_{38}$Sr	9014	4830	−2.631	−2.618	0.577	5.5	$7.58^{-4.32}_{+9.04}$
$^{98}_{39}$Y	8992	2576.6	−0.601	−0.578	0.571	0.33	$1.20^{-0.70}_{+1.65}$
$^{99}_{39}$Y	6971	2566	0.391	−0.277	0.569	1.97	$2.21^{-1.28}_{+2.97}$
$^{100}_{39}$Y	9050	2222	−0.312	−0.605	0.571	1.02	$0.61^{-0.36}_{+0.85}$
$^{101}_{39}$Y	8105	3245	−0.839	−0.992	0.569	1.98	$3.18^{-1.83}_{+4.15}$
$^{102}_{39}$Y	10414.5	3921.5	−1.204	−1.303	0.571	4	$3.91^{-2.25}_{+5.03}$
$^{103}_{39}$Y	9358	5059	−1.444	−1.749	0.568	8.1	$11.07^{-6.14}_{+11.93}$
$^{104}_{39}$Y	11660	5680	−1.551	−1.918	0.57	34	$11.32^{-6.29}_{+12.21}$
$^{106}_{41}$Nb	9931	3062.5	0.013	−1.088	0.571	4.5	$1.65^{-0.96}_{+2.24}$
$^{107}_{41}$Nb	8828	4339	−1.248	−1.47	0.569	7.4	$7.54^{-4.26}_{+8.84}$
$^{108}_{41}$Nb	11210	4934	−1.65	−1.723	0.57	6.3	$7.53^{-4.26}_{+8.87}$
$^{109}_{41}$Nb	9980	5990	−2.18	−2.147	0.568	31	$16.53^{-8.90}_{+15.66}$
$^{110}_{41}$Nb	12230	6280	−2.59	−2.207	0.57	40	$13.90^{-7.62}_{+14.11}$
$^{109}_{42}$Mo	7617	1185	−0.368	−0.719	0.569	1.3	$0.05^{-0.03}_{+0.07}$
$^{110}_{42}$Mo	6492	1669	−1.248	−1.077	0.579	2	$0.31^{-0.19}_{+0.45}$
$^{109}_{43}$Tc	6456	1307	−0.117	0.035	0.569	0.08	$0.16^{-0.09}_{+0.23}$
$^{110}_{43}$Tc	9038	1633	−0.093	−0.659	0.571	0.04	$0.16^{-0.09}_{+0.23}$
$^{111}_{43}$Tc	7761	2977	−1.224	−0.848	0.569	0.85	$2.64^{-1.53}_{+3.50}$
$^{112}_{43}$Tc	10372	3455	−1.187	−1.333	0.571	1.7	$2.31^{-1.34}_{+3.08}$
$^{113}_{43}$Tc	9057	4748	−1.884	−1.646	0.568	2.1	$9.79^{-5.47}_{+10.88}$
$^{114}_{43}$Tc	11620	5200	−2.408	−1.932	0.57	1.3	$8.06^{-4.55}_{+9.38}$
$^{118}_{45}$Rh	10501	3466	−1.255	−1.366	0.57	3.1	$2.31^{-1.34}_{+3.08}$
$^{119}_{45}$Rh	8585	4494.6	−1.661	−1.318	0.568	6.4	$10.48^{-5.83}_{+11.44}$
$^{123}_{46}$Pd	9120	2610	−2.226	−0.862	0.571	10	$1.27^{-0.74}_{+1.76}$
$^{124}_{46}$Pd	7810	3090	−2.513	−1.056	0.579	17	$4.12^{-2.37}_{+5.29}$
$^{125}_{46}$Pd	10400	4010	−2.813	−1.135	0.575	12	$6.03^{-3.44}_{+7.37}$
$^{126}_{46}$Pd	8820	4590	−3.024	−1.396	0.579	22	$15.74^{-8.55}_{+15.31}$
$^{121}_{47}$Ag	6671	1483	−0.252	0.408	0.57	0.08	$0.36^{-0.22}_{+0.53}$
$^{122}_{47}$Ag	9506	1896	−0.637	−0.232	0.571	0.186	$0.41^{-0.24}_{+0.57}$
$^{123}_{47}$Ag	7866	2993	−1.217	−0.113	0.572	0.56	$4.68^{-2.68}_{+5.89}$
$^{124}_{47}$Ag	10500	3140	−1.655	−0.428	0.573	1.3	$2.97^{-1.71}_{+3.87}$
$^{125}_{47}$Ag	8830	4110	−1.833	−0.449	0.573	11.8	$12.9^{-7.09}_{+13.33}$
$^{127}_{47}$Ag	10310	5750	−2.477	−1.145	0.574	14.6	$27.92^{-14.01}_{+20.22}$
$^{128}_{47}$Ag	12620	6060	−2.813	−1.136	0.573	20	$25.34^{-12.94}_{+19.53}$
$^{130}_{48}$Cd	8766	3649	−2.064	−1.163	0.583	3.5	$7.13^{-4.06}_{+8.54}$
$^{131}_{48}$Cd	12810	6590	−2.489	−2.043	0.575	3.5	$22.19^{-11.58}_{+18.46}$
$^{132}_{48}$Cd	12150	9690	−2.477	−3.522	0.582	60	$57.31^{-21.35}_{+18.93}$
$^{128}_{49}$In	9220	1250	−0.174	0.614	0.578	0.0384	$0.12^{-0.07}_{+0.18}$
$^{129}_{49}$In	7753	2453	−0.496	0.528	0.58	0.23	$3.19^{-1.85}_{+4.24}$

Table 4 (continued)

Nucl.	Q_β	$Q_{\beta n}$	$\ln T_{\mathrm{exp}}$	$\ln T_{\mathrm{cal}}$	$\sigma_{\ln T_{\mathrm{cal}}}$	$P_{\mathrm{exp}}(\%)$	$P_{\mathrm{cal}}(\%)$
$^{130}_{49}$In	10249	2636	−1.291	0.11	0.578	1.2	$2.1^{-1.22}_{+2.84}$
$^{131}_{49}$In	9239.5	4035.9	−1.324	−0.382	0.577	2.21	$12.19^{-6.75}_{+12.89}$
$^{132}_{49}$In	14135	6782	−1.603	−1.691	0.573	12.3	$25.53^{-13.02}_{+19.59}$
$^{133}_{49}$In	13410	11010	−1.82	−3.251	0.575	90	$69.46^{-20.61}_{+14.96}$
$^{133}_{50}$Sn	8049.6	690.1	0.351	0.38	0.581	0.0294	$0.01^{-0.01}_{+0.02}$
$^{134}_{50}$Sn	7586.8	4418.4	−0.103	−0.73	0.579	17	$25.45^{-13.03}_{+19.66}$
$^{135}_{50}$Sn	9058.1	5317	−0.662	−0.589	0.574	21	$34.03^{-16.31}_{+21.23}$
$^{136}_{50}$Sn	8610	5720	−1.064	−1.503	0.579	27	$37.98^{-17.66}_{+21.53}$
$^{137}_{50}$Sn	10270	6650	−1.444	−1.354	0.573	50	$44.37^{-19.35}_{+21.22}$
$^{135}_{51}$Sb	8038.5	4772.1	0.512	−0.071	0.573	20	$35.01^{-16.64}_{+21.32}$
$^{136}_{51}$Sb	9918.4	5150.6	−0.079	−0.159	0.572	25.14	$32.46^{-15.75}_{+21.06}$
$^{137}_{51}$Sb	9243	6294	−0.681	−1.006	0.573	49	$49.27^{-20.36}_{+20.60}$
$^{138}_{51}$Sb	11500	7000	−1.1	−1.18	0.571	72	$48.66^{-20.26}_{+20.71}$
$^{139}_{51}$Sb	10420	7840	−1.704	−1.85	0.573	90	$59.42^{-21.37}_{+18.31}$
$^{140}_{51}$Sb	12640	8200	−1.772	−1.816	0.571	30.6	$54.76^{-21.12}_{+19.53}$
$^{138}_{52}$Te	6283.9	2589	0.378	0.195	0.581	4.82	$6.21^{-3.54}_{+7.59}$
$^{140}_{53}$I	9380	3967	−0.528	−0.085	0.571	7.88	$12.47^{-6.86}_{+12.98}$
$^{141}_{53}$I	8271	4988	−0.868	−0.707	0.569	21.2	$27.50^{-13.80}_{+20.05}$
$^{141}_{54}$Xe	6280.2	781.5	0.547	0.779	0.572	0.0433	$0.03^{-0.02}_{+0.05}$
$^{142}_{54}$Xe	5284.9	1176.6	0.2	0.278	0.578	0.36	$0.25^{-0.15}_{+0.36}$
$^{143}_{54}$Xe	7472.6	2240.4	−0.671	−0.402	0.569	1	$1.21^{-0.71}_{+1.68}$
$^{144}_{54}$Xe	6399	2731.9	−0.947	−0.937	0.577	3	$3.54^{-2.05}_{+4.63}$
$^{145}_{54}$Xe	8561	3707	−1.671	−1.314	0.569	5	$5.04^{-2.88}_{+6.27}$
$^{146}_{54}$Xe	7355	4028	−1.924	−1.811	0.576	6.9	$8.93^{-5.04}_{+10.29}$
$^{142}_{55}$Cs	7327.7	1146.8	0.523	0.692	0.57	0.0916	$0.12^{-0.07}_{+0.18}$
$^{143}_{55}$Cs	6261.7	2095.4	0.585	0.328	0.569	1.582	$1.86^{-1.08}_{+2.52}$
$^{144}_{55}$Cs	8496	2595	−0.011	−0.357	0.57	2.98	$1.83^{-1.06}_{+2.47}$
$^{145}_{55}$Cs	7462	3641	−0.541	−0.784	0.568	13.5	$7.89^{-4.44}_{+9.16}$
$^{146}_{55}$Cs	9637	4134.5	−1.134	−1.155	0.57	14.3	$7.04^{-3.99}_{+8.38}$
$^{147}_{55}$Cs	8344	4956	−1.472	−1.485	0.568	28.5	$16.16^{-8.72}_{+15.44}$
$^{148}_{55}$Cs	10683	5282	−1.89	−1.744	0.57	29	$12.09^{-6.69}_{+12.80}$
$^{149}_{55}$Cs	9870	6270	−2.235	−2.349	0.568	25	$20.36^{-10.72}_{+17.63}$
$^{150}_{55}$Cs	11730	6880	−2.513	−2.326	0.569	20	$22.58^{-11.78}_{+18.67}$
$^{147}_{56}$Ba	6414	715	−0.112	−0.115	0.569	0.066	$0.01^{-0.01}_{+0.02}$
$^{148}_{56}$Ba	5115	1013	−0.483	−0.184	0.579	0.39	$0.10^{-0.06}_{+0.15}$
$^{149}_{56}$Ba	7100	1520	−1.044	−0.602	0.569	2.2	$0.20^{-0.12}_{+0.30}$
$^{148}_{57}$La	7690	1234	0.293	−0.104	0.571	0.19	$0.09^{-0.05}_{+0.13}$
$^{149}_{57}$La	6450	2110	0.087	−0.182	0.569	1.41	$1.32^{-0.77}_{+1.82}$
$^{150}_{57}$La	8720	2470	−0.673	−0.709	0.571	2.69	$1.14^{-0.66}_{+1.57}$

Table 5 Predictions of the half-life and probability for 123 nuclei corresponding to Eq. (4) and Eq. (10). The experimental and predicted half-lives are in the logarithmic scale, Q_β and $Q_{\beta n}$ are the decay energy of β-decay and βn -decay, respectively, in keV. The uncertainties are given in one standard deviation, estimated using the bootstrap method

Nucl.	Q_β	$Q_{\beta n}$	$\ln T_{\mathrm{exp}}$	$\ln T_{\mathrm{pred}}$	$\sigma_{\ln T_{\mathrm{pred}}}$	$P_{\mathrm{cal}}(\%)$
$^{82}_{29}$Cu	16990	12810	−3.433	−2.444	0.517	$69.09^{-21.29}_{+15.36}$
$^{78}_{30}$Zn	6222.7	437.8	0.385	0.750	0.522	0
$^{87}_{32}$Ge	11540	6810	−2.271	−1.383	0.514	$34.71^{-16.65}_{+21.53}$
$^{88}_{32}$Ge	10580	7410	−2.800	−1.914	0.523	$43.62^{-19.54}_{+21.78}$
$^{88}_{33}$As	13160	7640	−1.609	−1.154	0.518	$43.59^{-19.41}_{+21.61}$
$^{90}_{34}$Se	8200	4400	−1.635	−0.886	0.520	$16.12^{-8.70}_{+15.56}$
$^{100}_{36}$Kr	11200	8000	−4.962	−3.289	0.518	$22.99^{-12.03}_{+19.20}$
$^{103}_{37}$Rb	13810	10480	−3.772	−3.395	0.511	$36.03^{-17.08}_{+21.58}$
$^{96}_{38}$Sr	5411.7	213	0.067	0.333	0.518	0
$^{103}_{38}$Sr	11040	5680	−2.937	−2.292	0.511	$9.15^{-5.09}_{+10.29}$
$^{104}_{38}$Sr	9960	6280	−2.937	−2.743	0.518	$14.60^{-7.95}_{+14.74}$
$^{105}_{38}$Sr	12700	7380	−3.244	−2.993	0.511	$14.73^{-7.99}_{+14.57}$
$^{106}_{38}$Sr	11260	8400	−3.912	−3.356	0.518	$26.42^{-13.56}_{+20.39}$
$^{106}_{39}$Y	12500	7340	−2.501	−1.986	0.513	$22.86^{-11.91}_{+18.93}$
$^{107}_{39}$Y	12000	8110	−3.396	−2.726	0.511	$25.22^{-12.89}_{+19.57}$
$^{108}_{39}$Y	14060	9000	−3.507	−2.574	0.513	$30.26^{-15.07}_{+21.09}$
$^{109}_{39}$Y	12990	10080	−3.689	−3.122	0.511	$38.33^{-17.83}_{+21.68}$
$^{108}_{40}$Zr	8190	4300	−2.545	−1.797	0.518	$7.06^{-3.97}_{+8.44}$
$^{109}_{40}$Zr	10500	5280	−2.882	−2.075	0.511	$8.34^{-4.66}_{+9.56}$
$^{110}_{40}$Zr	9400	5730	−3.283	−2.486	0.518	$12.83^{-7.04}_{+13.48}$
$^{111}_{40}$Zr	11320	6700	−3.730	−2.451	0.511	$15.79^{-8.51}_{+15.24}$
$^{112}_{40}$Zr	10460	6990	−3.507	−3.021	0.518	$18.1^{-9.70}_{+16.90}$
$^{103}_{41}$Nb	5932	466.1	0.307	0.764	0.511	0
$^{111}_{41}$Nb	11060	7600	−2.919	−2.351	0.511	$26.64^{-13.50}_{+19.99}$
$^{112}_{41}$Nb	13190	7600	−3.270	−2.288	0.513	$21.42^{-11.24}_{+18.33}$
$^{113}_{41}$Nb	11980	8880	−3.442	−2.750	0.511	$33.67^{-16.25}_{+21.37}$
$^{114}_{41}$Nb	14420	9030	−4.075	−2.734	0.513	$28.25^{-14.25}_{+20.65}$
$^{115}_{41}$Nb	13400	10380	−3.772	−3.310	0.511	$38.15^{-17.78}_{+21.68}$
$^{112}_{42}$Mo	7800	3490	−2.079	−1.586	0.518	$3.60^{-2.05}_{+4.66}$
$^{113}_{42}$Mo	10320	4700	−2.526	−2.021	0.511	$5.55^{-3.14}_{+6.79}$
$^{114}_{42}$Mo	8790	4930	−2.847	−2.184	0.518	$9.24^{-5.15}_{+10.52}$
$^{115}_{42}$Mo	11570	5780	−3.090	−2.592	0.511	$8.13^{-4.54}_{+9.36}$
$^{116}_{42}$Mo	9960	6750	−3.442	−2.807	0.518	$19.06^{-10.17}_{+17.41}$
$^{117}_{42}$Mo	12210	7210	−3.817	−2.855	0.511	$15.74^{-8.49}_{+15.21}$
$^{118}_{42}$Mo	11160	7680	−3.963	−3.351	0.518	$20.52^{-10.87}_{+18.12}$
$^{115}_{43}$Tc	9870	5830	−2.551	−1.813	0.511	$15.67^{-8.45}_{+15.17}$
$^{116}_{43}$Tc	12610	6660	−2.865	−2.093	0.513	$15.66^{-8.47}_{+15.27}$
$^{117}_{43}$Tc	11110	7620	−3.112	−2.399	0.511	$26.61^{-13.48}_{+19.98}$
$^{118}_{43}$Tc	13470	7630	−3.507	−2.403	0.513	$20.54^{-10.83}_{+17.92}$
$^{119}_{43}$Tc	12190	8820	−3.817	−2.808	0.511	$32.68^{-15.88}_{+21.22}$
$^{120}_{43}$Tc	14490	8980	−3.863	−2.645	0.513	$30.35^{-15.07}_{+21.02}$
$^{121}_{43}$Tc	13270	10160	−3.817	−3.001	0.510	$44.15^{-19.42}_{+21.40}$
$^{114}_{44}$Ru	5489	474.4	−0.611	0.139	0.518	0
$^{115}_{44}$Ru	8040	1450	−1.146	−0.803	0.511	$0.10^{-0.06}_{+0.14}$
$^{116}_{44}$Ru	6667	2089.6	−1.590	−0.830	0.518	$0.77^{-0.44}_{+1.07}$
$^{117}_{44}$Ru	9410	3170	−1.890	−1.582	0.511	$1.54^{-0.88}_{+2.08}$
$^{118}_{44}$Ru	7630	3570	−2.313	−1.482	0.518	$4.47^{-2.54}_{+5.66}$

Table 5 (continued)

Nucl.	Q_β	$Q_{\beta n}$	$\ln T_{\mathrm{exp}}$	$\ln T_{\mathrm{pred}}$	$\sigma_{\ln T_{\mathrm{pred}}}$	$P_{\mathrm{cal}}(\%)$
$^{119}_{44}$Ru	10260	4250	−2.666	−1.962	0.511	$3.95^{-2.25}_{+5.01}$
$^{120}_{44}$Ru	8800	4740	−3.101	−2.092	0.518	$8.84^{-4.93}_{+10.12}$
$^{121}_{44}$Ru	11200	5700	−3.540	−2.218	0.510	$10.96^{-6.05}_{+11.79}$
$^{122}_{44}$Ru	9930	6030	−3.689	−2.416	0.518	$17.97^{-9.61}_{+16.66}$
$^{123}_{44}$Ru	12280	6930	−3.963	−2.310	0.510	$22.13^{-11.51}_{+18.39}$
$^{124}_{44}$Ru	10930	7330	−4.200	−2.489	0.520	$33.99^{-16.47}_{+21.61}$
$^{115}_{45}$Rh	6197	1190	0.030	0.485	0.511	$0.13^{-0.08}_{+0.19}$
$^{121}_{45}$Rh	9930	5960	−2.577	−1.632	0.510	$20.36^{-10.70}_{+17.63}$
$^{122}_{45}$Rh	12540	6030	−2.976	−1.721	0.513	$15.22^{-8.23}_{+14.88}$
$^{123}_{45}$Rh	11070	7190	−3.170	−1.877	0.510	$33.01^{-15.96}_{+21.18}$
$^{124}_{45}$Rh	13500	7470	−3.507	−1.751	0.515	$32.14^{-15.69}_{+21.18}$
$^{125}_{45}$Rh	12120	8320	−3.631	−1.997	0.512	$46.99^{-20.12}_{+21.16}$
$^{126}_{45}$Rh	14560	8750	−3.963	−1.858	0.518	$47.36^{-20.31}_{+21.23}$
$^{127}_{45}$Rh	13150	9760	−3.912	−2.252	0.514	$59.36^{-21.77}_{+18.60}$
$^{119}_{46}$Pd	7238	74.6	−0.083	−0.181	0.510	0
$^{120}_{46}$Pd	5371.5	294	−0.709	0.415	0.518	0
$^{121}_{46}$Pd	8220	1397.9	−1.238	−0.653	0.510	$0.10^{-0.06}_{+0.15}$
$^{122}_{46}$Pd	6490	1715	−1.645	−0.321	0.518	$0.55^{-0.31}_{+0.76}$
$^{128}_{46}$Pd	10130	5880	−3.352	−1.929	0.523	$25.28^{-12.99}_{+19.80}$
$^{129}_{46}$Pd	14370	8940	−3.474	−2.738	0.513	$39.52^{-18.22}_{+21.72}$
$^{130}_{47}$Ag	15420	9290	−3.194	−2.151	0.519	$48.29^{-20.51}_{+21.11}$
$^{131}_{47}$Ag	14840	12670	−3.352	−2.946	0.513	$71.84^{-20.58}_{+14.20}$
$^{132}_{47}$Ag	16470	13360	−3.576	−2.590	0.517	$75.48^{-19.73}_{+12.71}$
$^{126}_{48}$Cd	5516	149	−0.666	0.980	0.521	0
$^{127}_{48}$Cd	8149	954	−0.799	0.036	0.513	$0.04^{-0.02}_{+0.06}$
$^{128}_{48}$Cd	6900	1583	−1.402	−0.065	0.522	$0.54^{-0.31}_{+0.76}$
$^{129}_{48}$Cd	9780	3020	−1.890	−0.825	0.514	$2.94^{-1.68}_{+3.87}$
$^{133}_{48}$Cd	13540	10420	−2.749	−2.502	0.513	$61.77^{-21.77}_{+17.86}$
$^{134}_{48}$Cd	12740	10470	−2.733	−3.206	0.521	$58.49^{-22.00}_{+19.03}$
$^{135}_{49}$In	14100	11830	−2.293	−2.689	0.513	$70.92^{-20.80}_{+14.58}$
$^{136}_{49}$In	15390	12050	−2.465	−2.197	0.518	$74.18^{-20.15}_{+13.28}$
$^{137}_{49}$In	14750	12790	−2.733	−2.946	0.513	$73.19^{-20.24}_{+13.64}$
$^{138}_{50}$Sn	9400	7130	−1.871	−1.616	0.523	$52.33^{-21.38}_{+20.55}$
$^{139}_{50}$Sn	11350	7700	−2.120	−1.593	0.514	$49.58^{-20.70}_{+20.85}$
$^{134}_{51}$Sb	8513.2	845.3	−0.393	0.772	0.519	$0.03^{-0.02}_{+0.05}$
$^{141}_{51}$Sb	11380	9400	−2.273	−1.721	0.513	$67.87^{-21.30}_{+15.75}$
$^{139}_{52}$Te	8265.9	3703.5	−0.298	−0.189	0.512	$11.86^{-6.52}_{+12.56}$
$^{140}_{52}$Te	7030	3823	−1.047	−0.404	0.520	$16.94^{-9.10}_{+16.05}$
$^{141}_{52}$Te	9440	5050	−1.645	−0.978	0.511	$20.57^{-10.80}_{+17.76}$
$^{142}_{52}$Te	8400	5490	−1.917	−1.428	0.519	$28.61^{-14.39}_{+20.69}$
$^{143}_{52}$Te	10350	6420	−2.120	−1.577	0.510	$30.16^{-14.89}_{+20.74}$
$^{142}_{53}$I	10460	5360	−1.448	−0.806	0.514	$21.38^{-11.18}_{+18.14}$
$^{143}_{53}$I	9570	6530	−1.704	−1.403	0.510	$34.84^{-16.61}_{+21.37}$
$^{144}_{53}$I	11590	6850	−2.364	−1.506	0.513	$29.69^{-14.77}_{+20.81}$
$^{145}_{53}$I	10550	7860	−2.411	−2.056	0.510	$39.97^{-18.28}_{+21.60}$
$^{148}_{54}$Xe	8310	5250	−2.465	−2.060	0.518	$15.04^{-8.17}_{+15.03}$
$^{151}_{55}$Cs	10710	7600	−2.830	−2.403	0.511	$29.52^{-14.67}_{+20.70}$

Table 5 (continued)

Nucl.	Q_β	$Q_{\beta n}$	$\ln T_{\mathrm{exp}}$	$\ln T_{\mathrm{pred}}$	$\sigma_{\ln T_{\mathrm{pred}}}$	$P_{\mathrm{cal}}(\%)$
$^{150}_{56}$Ba	6230	2250	−1.355	−0.674	0.518	$1.43^{-0.82}_{+1.94}$
$^{151}_{56}$Ba	8370	3120	−1.790	−1.185	0.511	$2.36^{-1.35}_{+3.12}$
$^{152}_{56}$Ba	7580	3530	−1.966	−1.655	0.518	$4.27^{-2.43}_{+5.44}$
$^{153}_{56}$Ba	9590	4750	−2.180	−1.866	0.511	$7.85^{-4.39}_{+9.10}$
$^{154}_{56}$Ba	8710	5170	−2.937	−2.350	0.518	$11.57^{-6.39}_{+12.51}$
$^{151}_{57}$La	7910	3470	−0.783	−0.917	0.511	$4.74^{-2.69}_{+5.91}$
$^{152}_{57}$La	9690	3860	−1.211	−0.988	0.513	$5.03^{-2.85}_{+6.25}$
$^{153}_{57}$La	8850	4850	−1.406	−1.478	0.511	$11.76^{-6.47}_{+12.45}$
$^{154}_{57}$La	10690	5310	−1.826	−1.479	0.513	$12.37^{-6.79}_{+13.00}$
$^{155}_{57}$La	9850	6220	−2.293	−2.014	0.511	$19.98^{-10.53}_{+17.51}$
$^{156}_{57}$La	11770	6660	−2.477	−1.961	0.513	$20.1^{-10.62}_{+17.73}$
$^{85}_{30}$Zn	14620	10790	-	−2.682	0.512	$54.96^{-21.41}_{+19.71}$
$^{89}_{32}$Ge	13070	8920	-	−2.005	0.514	$50.23^{-20.82}_{+20.73}$
$^{90}_{32}$Ge	12110	9510	-	−2.589	0.523	$56.10^{-21.84}_{+19.68}$
$^{89}_{33}$As	12190	9020	-	−1.732	0.513	$57.61^{-21.66}_{+19.07}$
$^{90}_{33}$As	14470	9590	-	−1.666	0.518	$57.12^{-21.75}_{+19.28}$
$^{91}_{33}$As	13680	10830	-	−2.351	0.513	$63.67^{-21.69}_{+17.23}$
$^{92}_{33}$As	15740	11530	-	−2.134	0.517	$66.32^{-21.65}_{+16.39}$
$^{92}_{34}$Se	9510	6310	-	−1.761	0.519	$29.99^{-14.94}_{+20.99}$
$^{93}_{34}$Se	12180	7450	-	−2.103	0.510	$28.87^{-14.38}_{+20.47}$
$^{94}_{34}$Se	10600	8020	-	−2.444	0.518	$39.83^{-18.46}_{+21.94}$
$^{95}_{34}$Se	13310	8870	-	−2.685	0.510	$33.98^{-16.31}_{+21.29}$
$^{95}_{35}$Br	12390	9510	-	−2.575	0.510	$43.17^{-19.18}_{+21.48}$
$^{96}_{35}$Br	14920	9920	-	−2.624	0.513	$38.11^{-17.87}_{+21.84}$
$^{97}_{35}$Br	13370	10950	-	−3.070	0.510	$47.37^{-20.20}_{+21.11}$
$^{98}_{35}$Br	16060	11100	-	−3.082	0.513	$40.00^{-18.50}_{+21.91}$
$^{101}_{36}$Kr	13720	9050	-	−3.342	0.511	$23.31^{-12.05}_{+18.91}$
$^{107}_{38}$Sr	13470	9080	-	−3.287	0.511	$25.01^{-12.80}_{+19.50}$
$^{152}_{55}$Cs	12780	7940	-	−2.344	0.513	$27.55^{-13.96}_{+20.47}$

Acknowledgements Discussions with Mr. Guang-Shang Chen, Jiong-Yu Xu, and Bo-Cong Liu are greatly appreciated.

Author Contributions All authors contributed to the study conception and design. Material preparation, data collection and analysis were performed by Yu-Feng Gao and Bo-Shuai Cai. The first draft of the manuscript was written by Yu-Feng Gao and all authors commented on previous versions of the manuscript. All authors read and approved the final manuscript.

References

1. R. Barton, R. Mcpherson, R.E. Bell et al., Observation of delayed proton radioactivity. Can. J. Phys. **41**, 2007–2025 (1963). https://doi.org/10.1139/p63-201
2. M.D. Cable, J. Honkanen, R.F. Parry et al., Discovery of beta-delayed two-proton radioactivity: ^{22}Al. Phys. Rev. Lett. **50**, 404–406 (1983). https://doi.org/10.1103/PhysRevLett.50.404
3. K. Miernik, W. Dominik, Z. Janas et al., First observation of β-delayed three-proton emission in ^{45}Fe. Phys. Rev. C **76**, 041304 (2007). https://doi.org/10.1103/PhysRevC.76.041304
4. N. Frédéric, O. Alexandre, P. Alfredo, The neutron-rich edge of the nuclear landscape: experiment and theory. Prog. Part. Nucl. Phys. **120**, 103866 (2021). https://doi.org/10.1016/j.ppnp.2021.103866
5. X.P. Zhang, Z.Z. Ren, Q.J. Zhi et al., Systematics of β^{-}-decay half-lives of nuclei far from the β-stable line. J. Phys. G: Nucl. Part. Phys. **34**, 2611–2632 (2007). https://doi.org/10.1088/0954-3899/34/12/007
6. D.Z. Chen, D.L. Fang, C.L. Bai, Impact of finite-range tensor terms in the Gogny force on the β-decay of magic nuclei. Nucl. Sci. Tech. **32**, 74 (2021). https://doi.org/10.1007/s41365-021-00908-9
7. X. Zhou, M. Wang, Y.H. Zhang et al., Charge resolution in the isochronous mass spectrometry and the mass of ^{51}Co. Nucl. Sci. Tech. **32**, 37 (2021). https://doi.org/10.1007/s41365-021-00876-0
8. W. Nan, B. Bing, C.J. Lin et al., First proof-of-principle experiment with the post-accelerated isotope separator on-line beam at BRIF: measurement of the angular distribution of ^{23}Na + ^{40}Ca

elastic scattering. Nucl. Sci. Tech. **32**, 53 (2021). https://doi.org/10.1007/s41365-021-00889-9
9. S.W. Bai, X.F. Yang, S.J. Wang et al., Commissioning of a high-resolution collinear laser spectroscopy apparatus with a laser ablation ion source. Nucl. Sci. Tech. **33**, 9 (2022). https://doi.org/10.1007/s41365-022-00992-5
10. W. Liu, J.L. Lou, Y.L. Ye et al., Experimental study of intruder components in light neutron-rich nuclei via single-nucleon transfer reaction. Nucl. Sci. Tech. **31**, 20 (2020). https://doi.org/10.1007/s41365-020-0731-y
11. Z.P. Gao, Y.J. Wang, H.L. Lü et al., Machine learning the nuclear mass. Nucl. Sci. Tech. **32**, 109 (2021). https://doi.org/10.1007/s41365-021-00956-1
12. L. Zhou, S.M. Wang, D.Q. Fang et al., Recent progress in two-proton radioactivity. Nucl. Sci. Tech. **33**, 105 (2022). https://doi.org/10.1007/s41365-022-01091-1
13. M.J.G. Borge, β-delayed particle emission. Phys. Scr. **T152**, 014013 (2013). https://doi.org/10.1088/0031-8949/2013/t152/014013
14. L. Zhou, D.Q. Fang, Effect of source size and emission time on the p-p momentum correlation function in the two-proton emission process. Nucl. Sci. Tech. **31**, 52 (2020). https://doi.org/10.1007/s41365-020-00759-w
15. H.C. Manjunatha, N. Sowmya, P.S. Damodara-Gupta et al., Investigation of decay modes of superheavy nuclei. Nucl. Sci. Tech. **32**, 130 (2021). https://doi.org/10.1007/s41365-021-00967-y
16. Z.X. Fang, M. Yu, Y.G. Huang et al., Theoretical analysis of long-lived radioactive waste in pressurized water reactor. Nucl. Sci. Tech. **32**, 72 (2021). https://doi.org/10.1007/s41365-021-00911-0
17. H.M. Şahin, G. Tunç, A. Karakoç et al., Neutronic study on the effect of first wall material thickness on tritium production and material damage in a fusion reactor. Nucl. Sci. Tech. **33**, 39–69 (2022). https://doi.org/10.1007/s41365-022-01029-7
18. J. Suhonen, Value of the axial-vector coupling strength in β and β decays: A review. Front. Phys. **5**, 55 (2017). https://doi.org/10.3389/fphy.2017.00055
19. A. Ravlić, E. Yüksel, Y.F. Niu et al., Evolution of β-decay half-lives in stellar environments. Phys. Rev. C **104**, 054318 (2021). https://doi.org/10.1103/PhysRevC.104.054318
20. F. Minato, T. Marketin, P. Nils, β-delayed neutron-emission and fission calculations within relativistic quasiparticle random-phase approximation and a statistical model. Phys. Rev. C **104**, 044321 (2021). https://doi.org/10.1103/PhysRevC.104.044321
21. Z.M. Niu, Y.F. Niu, H.Z. Liang et al., β-decay half-lives of neutron-rich nuclei and matter flow in the r-process. Phys. Lett. B **723**, 172–176 (2013). https://doi.org/10.1016/j.physletb.2013.04.048
22. P. Möller, M.R. Mumpower, T. Kawano, Nuclear properties for astrophysical and radioactive-ion-beam applications (II). Atom. Data Nucl. Data Tables **125**, 1–192 (2019). https://doi.org/10.1016/j.adt.2018.03.003
23. S. Yoshida, Y. Utsuno, N. Shimizu et al., Systematic shell-model study of β-decay properties and Gamow-Teller strength distributions in $A \approx 40$ neutron-rich nuclei. Phys. Rev. C **97**, 054321 (2018). https://doi.org/10.1103/PhysRevC.97.054321
24. E. Mardones, J. Barea, C.E. Alonso, β-decay rates of $^{121-131}$Cs in the microscopic interacting boson-fermion model. Phys. Rev. C **93**, 044306 (2016). https://doi.org/10.1103/PhysRevC.93.034332
25. J. Ferretti, J. Kotila, R.I. Vsevolodovna *et al.*, β-decay rates of ^{115,117}Rh into ^{115,117} Pd isotopes in the microscopic interacting boson-fermion model. Phys. Rev. C **102**, 054329 (2020). https://doi.org/10.1103/PhysRevC.102.054329
26. K. Nomura, β decay and evolution of low-lying structure in Ge and As nuclei. Phys. Rev. C **105**, 044306 (2022). https://doi.org/10.1103/PhysRevC.105.044306
27. I.N. Borzov, S. Goriely, J.M. Pearson, Microscopic calculations of β-decay characteristics near the $A = 130 r$-process peak. Nucl. Phys. A **81**, 044620 (2010). https://doi.org/10.1103/PhysRevC.81.044620
28. I.N. Borzov, J.J. Cuenca-García, K. Langanke et al., Beta-decay of $Z < 50$ nuclei near the $N = 82$ closed neutron shell. Nucl. Phys. A **814**, 159–173 (2008). https://doi.org/10.1016/j.nuclphysa.2008.09.010
29. J.J. Cuenca-García, G. Martínez-Pinedo, K. Langanke et al., Shell model half-lives for r-process $N = 82$ nuclei. Eur. Phys. J. A **34**, 99–105 (2007). https://doi.org/10.1140/epja/i2007-10477-3
30. K. Yoshida, Suddenly shortened half-lives beyond ^{78}Ni : $N = 50$ magic number and high-energy nonunique first-forbidden. Phys. Rev. C **100**, 024316 (2019). https://doi.org/10.1103/PhysRevC.100.024316
31. K. Miernik, Phenomenological model of β-delayed neutron-emission probability. Phys. Rev. C **88**, 041301 (2013). https://doi.org/10.1103/PhysRevC.88.041301
32. A.I. Morales, J. Benlliure, T. Kurtukián-Nieto et al., Half-Life Systematics across the $N = 126$ Shell closure: Role of first-forbidden transitions in the β decay of heavy neutron-rich nuclei. Phys. Rev. Lett. **113**, 022702 (2014). https://doi.org/10.1103/PhysRevLett.113.022702
33. Y. Zhou, Z.H. Li, Y.B. Wang et al., Empirical formula for β^--decay half-lives of r-process nuclei. Sci. China. Phys. Mech. Astron. **60**, 082012 (2017). https://doi.org/10.1007/s11433-017-9045-0
34. B. Pfeiffer, K.L. Kratz, P. Möller et al., Status of delayed-neutron precursor data: half-lives and neutron emission probabilities. Prog. Nucl. Energy **41**, 39–69 (2002). https://doi.org/10.1016/S0149-1970(02)00005-7
35. D. Benzaid, S. Bentridi, A. Kerraci et al., Bethe-Weizsäcker semiempirical mass formula coefficients 2019 update based on AME2016. Nucl. Sci. Tech. **31**, 9 (2020). https://doi.org/10.1007/s41365-019-0718-8
36. M. Wang, W. J. Huang, F. G. Kondev *et al.*, The AME 2020 atomic mass evaluation (II). Tables, graphs and references∗, Chinese Phys. C **45**, 030003 (2021). https://doi.org/10.1088/1674-1137/abddaf
37. G. Audi, A.H. Wapstra, C. Thibault, The AME2003 atomic mass evaluation: (II). Tables, graphs and references. Nucl. Phys. A **729**, 337–676 (2003). https://doi.org/10.1016/j.nuclphysa.2003.11.003
38. P. T. Hosmer, H. Schatz, A. Aprahamian, *et al.*, Half-Life of the doubly magic r-process nucleus ^{78}Ni. Phys. Rev. Lett. **94**, 112501. https://doi.org/10.1103/PhysRevLett.94.112501
39. R. Dunlop, V. Bildstein, I. Dillmann et al., Half-lives of neutron-rich $^{128-130}$Cd. Phys. Rev. C **93**, 062801 (2016). https://doi.org/10.1103/PhysRevC.93.062801
40. T. Marketin, L. Huther, G. Martínez-Pinedo, Large-scale evaluation of β-decay rates of r-process nuclei with the inclusion of first-forbidden transitions. Phys. Rev. C **93**, 025805 (2016). https://doi.org/10.1103/PhysRevC.93.025805
41. J.L. You, X.P. Zhang, Q.J. Zhi et al., The contribution of the first forbidden transitions to the nuclear β^--decay half-life. Chinese Phys. C **43**, 114104 (2019). https://doi.org/10.1088/1674-1137/43/11/114104
42. C.L. Lan, M. Peng, Y. Zhang et al., Possible cluster states in heavy and superheavy nuclei. Nucl. Sci. Tech. **104**, L031301 (2017). https://doi.org/10.1007/s41365-016-0158-7
43. J. Liang, B. Singh, E.A. McCutchan, I. Dillmann et al., Compilation and evaluation of β-delayed neutron emission probabilities and half-Lives for $Z > 28$ precursors. Nucl. Data Sheets **168**, 1–116 (2020). https://doi.org/10.1016/j.nds.2020.09.001
44. J. Suhonen, From nucleons to nucleus: Concepts of microscopic nuclear theory (Springer Science & Business Media, 2007), pp. 163–164

45. H. Primakoff, S.P. Rosen, Double beta decay. Rep. Prog. Phys. **22**, 121 (1959). https://doi.org/10.1088/0034-4885/22/1/305
46. B. Efron, R. Tibshirani, The bootstrap method for assessing statistical accuracy. Behaviormetrika **12**, 1–35 (1985). https://doi.org/10.2333/bhmk.12.17_1
47. B.S. Cai, G.S. Chen, J.Y. Xu et al., α decay half-life estimation and uncertainty analysis. Phys. Rev. C **101**, 054304 (2020). https://doi.org/10.1103/PhysRevC.101.054304
48. Y.P. Cao, D.H. Lu, Y.B. Qian et al., Uncertainty analysis for the nuclear liquid drop model and implications for the symmetry energy coefficients. Phys. Rev. C **105**, 034304 (2022). https://doi.org/10.1103/PhysRevC.105.034304
49. B.S. Cai, G.S. Chen, C.X. Yuan et al., Shell-model study on properties of proton dripline nuclides with $Z, N = 30 - 50$ including uncertainty analysis. Chinese Phys. C **46**, 084104 (2022). https://doi.org/10.1088/1674-1137/ac6cd7
50. J.H. Jia, Y.B. Qian, Z.Z. Ren, Possible cluster states in heavy and superheavy nuclei. Phys. Rev. C **104**, L031301 (2021). https://doi.org/10.1103/PhysRevC.104.L031301
51. G. Martínez-Pinedo, K. Langanke, Shell model applications in nuclear astrophysics. Physics **4**, 677–689 (2022). https://doi.org/10.3390/physics4020046
52. V.H. Phong, S. Nishimura, G. Lorusso et al., β-delayed one and two neutron emission probabilities southeast of ^{132}Sn and the odd-even systematics in r-process nuclide abundances. Phys. Rev. Lett. **129**, 172701 (2022). https://doi.org/10.1103/PhysRevLett.129.172701